# Room Temperature Synthesis of HgTe Quantum Dots in an Aprotic Solvent Realizing High Photoluminescence Quantum Yields in the Infrared.

Nema M. Abdelazim,[†] Qiang Zhu,[‡] Yuan Xiong,[†] Ye Zhu,[#] Mengyu Chen,[‡] Ni Zhao,[‡] Stephen V. Kershaw,[†] Andrey L. Rogach[†]

[†]Department of Physics and Materials Science and Centre for Functional Photonics (CFP), City University of Hong Kong, Kowloon, Hong Kong S. A. R.
[‡]Department of Electronic Engineering, The Chinese University of Hong Kong, Shatin, New Territories, Hong Kong S. A. R.
[#]Department of Applied Physics, The Hong Kong Polytechnic University, Kowloon, Hong Kong S. A. R.

**SI 1. Te electrode calibration**

The electrolyte was a 60 vol.% aqueous phosphoric acid solution. An inert gas flow (99.999% Argon) was used to degas the electrolyte and also to act as a carrier for the $H_2Te$. The electrolyte reactions are the same as for the electrolysis of water in acidified solution, with the modification that at the tellurium anode, a proportion of the hydrogen ions evolved can also react with the tellurium surface to form the gaseous dihydride. Neglecting the proportion of the protons that simply form $H_2$ gas, the anode and cathode reactions can be described as:

$$\mathrm{Te} + 2\,H^+ + 2\,e^- \rightarrow H_2Te \qquad (1)$$

$$4\,OH^- - 4\,e^- \rightarrow 2H_2O + O_2 \qquad (2)$$

In order to further minimize the $H_2Te$ decomposition in the cell, the whole set-up was immersed in a chiller (at 5 $^oC$). The quantity of $H_2Te$ gas can be easily calculated as follows:

$$\nu\ (\mathrm{mol}) = \frac{\mathrm{I\,t\,\eta}}{2\,\mathrm{F}} \qquad (3)$$

where I – current (A), t – time (s), η – current yield, F= 96485 $s \cdot A \cdot mol^{-1}$– Faraday constant. Using this equation, we can calculate the amount of $H_2Te$ passed through the solution over a given time, if the current yield of the cell is known. The current yield differed for each tellurium electrode, and is also a function of the electrolysis current and decreased as the electrodes and the electrolyte aged. Losses in the overall delivery of the $H_2Te$ gas into the reaction flask are also factored into η. The benefit of the electrochemical generation method is that the gas is only produced as needed and passed directly into the in-line reaction flask and moreover can be produced at low, controllable concentrations and over a programmable period of time.

To calibrate the electrolysis cell (i.e. determine η(I)), $H_2Te$ gas was passed into 30 mL solutions of 1M NaOH at various steady currents for measured time intervals. The Ar flow rate was regulated with a Bronkhorst mass flow controller and the same flow conditions used for both calibration and the syntheses described in the main text. After the electrolysis duration, the current was switched off and the Ar flow continued through the electrolysis cell and calibration sample for a further 15 minutes to clear any $H_2Te$ from the system. The sample tube containing the NaOH was then removed and allowed to stand in air allowing the absorbed $H_2Te$ (which forms a NaHTe solution) to decompose to form elemental Te precipitate. The more concentrated solutions took several days to fully decompose, with the initial intense purple color giving way to a clear solution with a solid Te precipitate in the base of

the tubes. Once the decomposition was fully complete, the Te precipitate was washed three times with milliQ water to remove any traces of NaOH by applying centrifugation several times. A final wash with methanol was then made to facilitate drying. After complete drying (no observable mass change) the mass of the Te was determined and used to calculate η(I). Figure S1 shows a typical set of calibration results. Under the conditions that were used in the syntheses described in the main paper, we found it best to recheck the calibration every two weeks. Heavier use may require more frequent checks and can be useful to both spot a failing electrode or to replace the electrolyte with fresh solution.

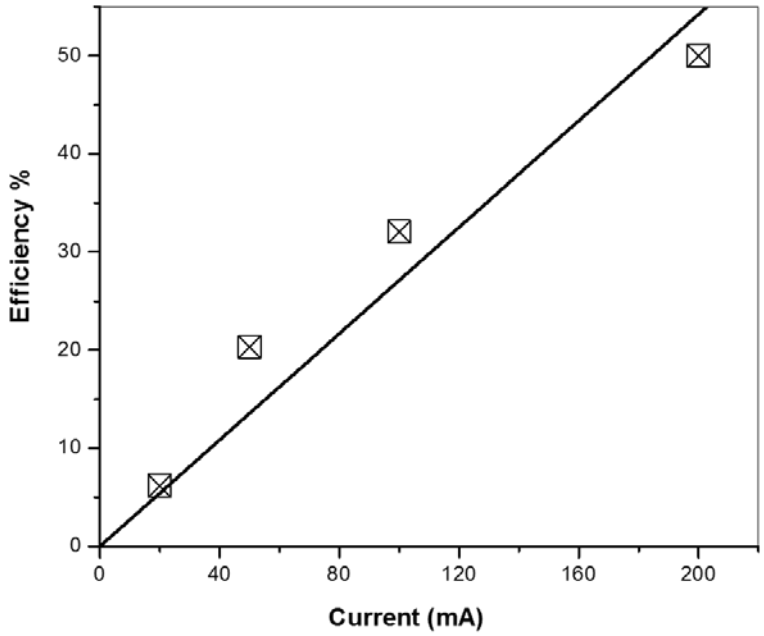


**Figure S1.** Typical efficiency (η) vs. current relationship for Te electrode electrolysis cell.

**SI.2 Measurement sequence and ligand and solvent exchange method (DMSO/FMT to TCE/DDT)**

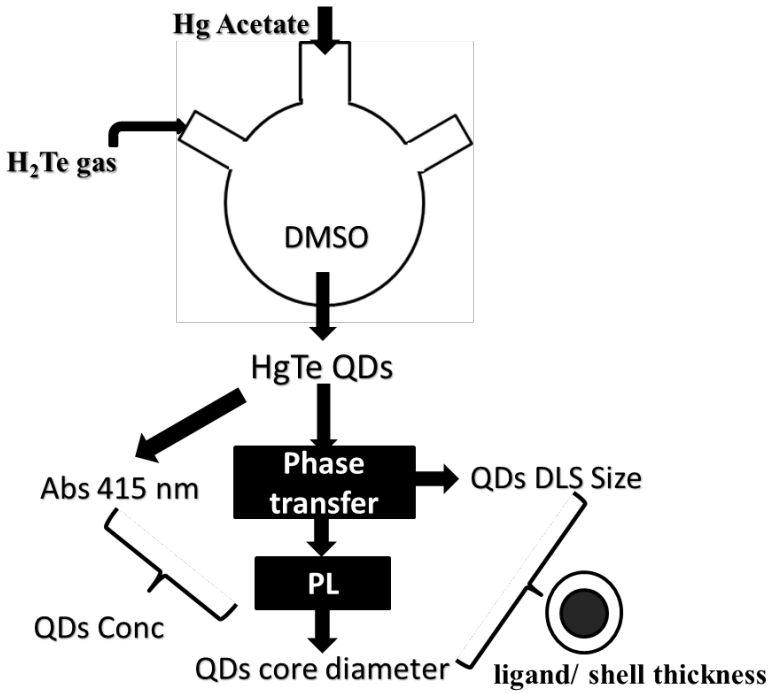


**Figure S2.** Overview of the steps used in the gas injection, room temperature method to control the rates of precursor addition to regulate the relative proportions of nucleation vs. growth. Absorption, PL and DLS measurements at intervals during measurement were used to determine particle size and concentration and to monitor for any signs of QD aggregation during the synthesis.

Evaluation of purification and phase transfer scheme

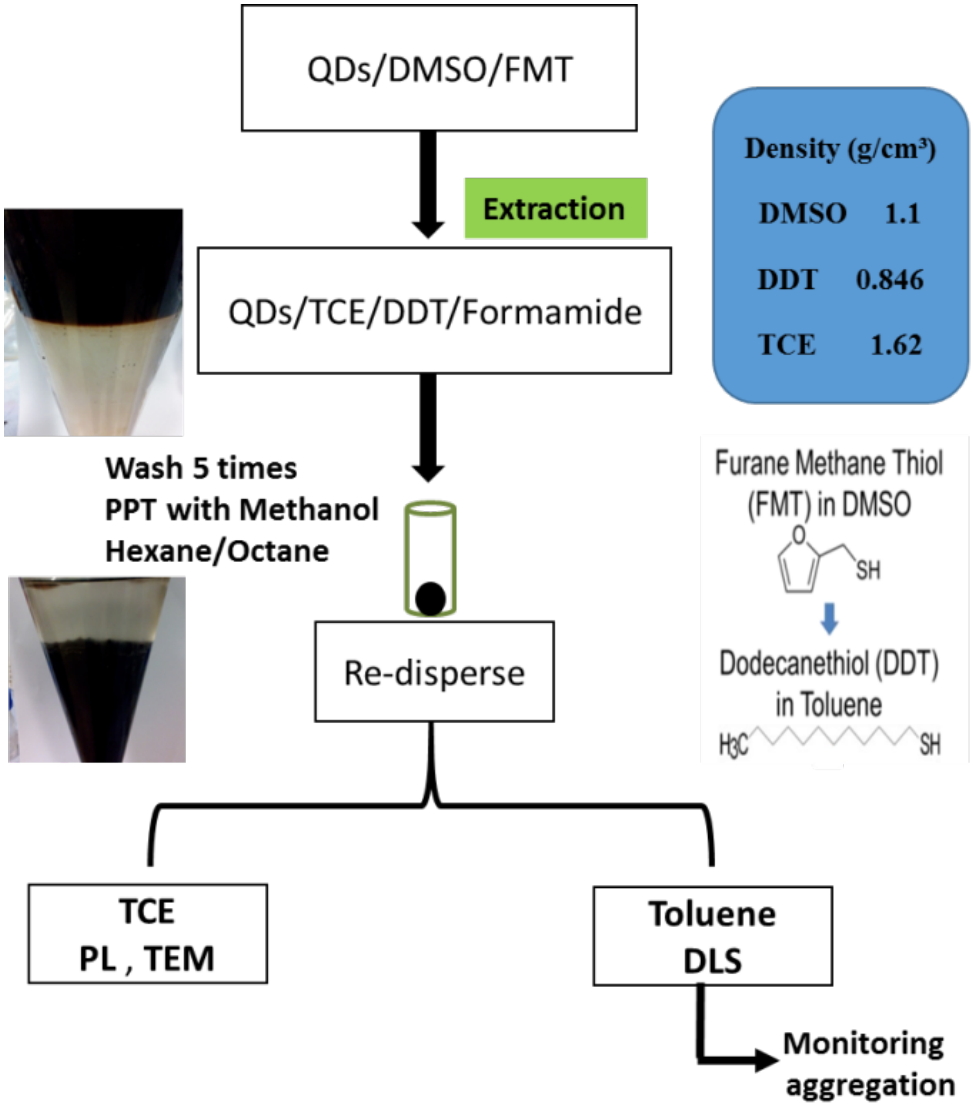


**Figure S3**. Schematic diagram of purification and transfer process used in this work.

The extraction method used to transfer QDs from DMSO/FMT solutions into TCE (or toluene)/ DDT solutions whilst also purifying them and discarding excess ligands used to effect the transfer is illustrated in figure S4.

We developed an effective washing method by changing the number of wash cycles after the initial transfer, systematically investigating the effect this had on particle size distributions using dynamic light scattering which measured the hydrodynamic particle diameters in solution. Up to ten wash cycles were used: initially there was a clear decrease in particle size after washing until between 5 to 7 washes, whilst after more than 7 washes the diameter started to increase again indicating depletion of the ligand below a sufficient level to prevent QD aggregation.

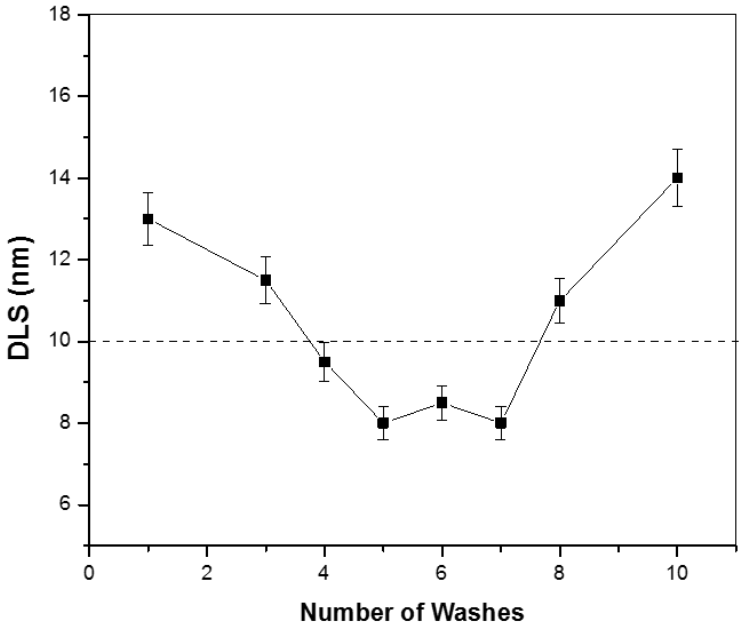


**Figure S4**. Optimization of the number of (methanol/precipitate/ re-dissolve in hexane/octane) washes using dynamic light scattering (DLS) measurements to follow the hydrodynamic diameter variation. Initially the hydrodynamic diameter is large due to the high excess of DDT used to drive the transfer from the DMSO-based solution. The dashed line shows the acceptable limit, which corresponds to aggregates of QDs with diameters equivalent to 2 dots each coated with a DDT layer. For 5-7 washes the DDT concentration is acceptable. For 8 washes and above, the DDT concentration was sufficiently depleted that QDs started to form aggregates.

**SI 3. Synthetic set-up and reaction sequence**

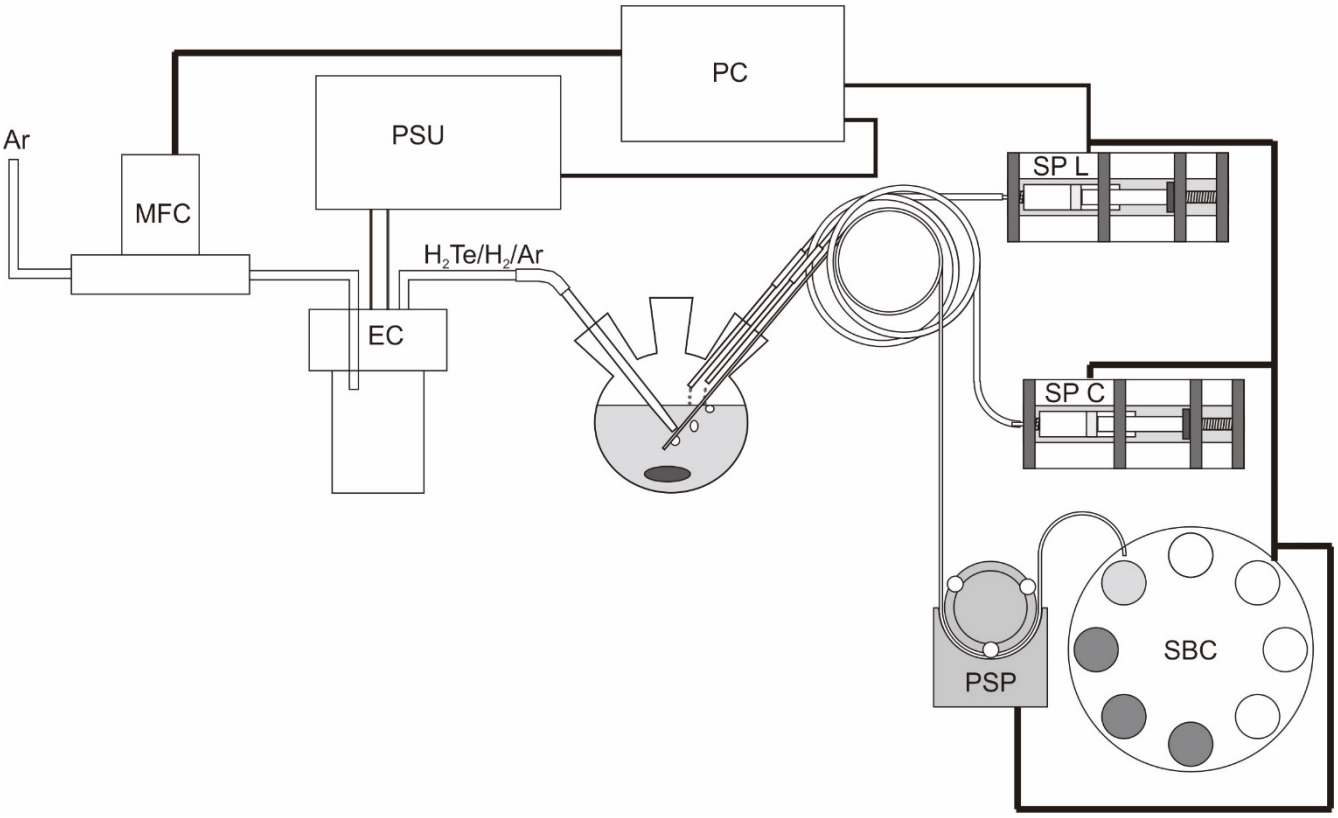


Ar – Argon gas inlet, MFC – programable mass flow controller, EC – electrochemical cell, PSU power supply unit for EC, PC – laptop computer running LabView, SP L – syringe pump with ligand solution, SP C – syringe pump with cation solution, PSP – peristaltic pump for automatic aliquot removal, SBC – sample bottle carousel.

Program sequence:

Set run parameters (number of loops, wait times, whether to add additional ligand or $Hg^{2+}$ salt, EC voltage limit, EC current, $H_2Te$ generation time, aliquot quantity, which loops to take aliquots).

Start loop

Add extra ligand? Y/N (optional)

Wait

Add extra $Hg^{2+}$ salt? Y/N (optional)

Wait

Run EC for X mins at Y current

Wait

Remove an aliquot on this loop? Y/N (optional)

Move sample bottle carousel round by one position (if aliquot removed)

Repeat loop

**Figure S5.** Automated synthesis set-up and generalized sequence of operations.

**SI 4. A simple method to estimate the amount of evaporation loss of FMT from the reaction mixture over extended time periods and as a function of Ar flow rate**

The FMT ligand is also a commercial food and beverage odorant additive (e.g. for coffee, etc) and has a moderate degree of volatility. For short duration syntheses (e.g. few hours) evaporation loss due to the flow of gases through the system would not be a significant problem, but for some of the slow iterative syntheses discussed in the main paper, reactions were continued for several days. Under these conditions, the FMT ligand must be periodically topped up to avoid significant depletion occurring. In order to determine the loss rate, we added a known and set amount of FMT to a flask containing DMSO solvent and passed Ar gas through it continuously for durations of up to 80 hours. The gas flow rate was regulated using a Bronkhorst mass flow controller and a number of runs at different flow rates were made. At measured time intervals, small samples were removed from the flask and these were then assayed for their FMT concentrations.

Thiol assays are commonplace in biochemistry and fluorimetric assay kits for water based thiol solutions are available commercially from several chemical suppliers. However, we found that these were not suitable for pure DMSO solvent based solutions. However, we did establish that the UV absorption arising primarily from FMT itself could be used to establish an absorption based assay. The following assay protocol based on Egwim and Gruber's work[1] was used:

A test solution (e.g. FMT/DMSO 1 ml) was first treated with 33.3µls of 1M NaOH solution and then incubated for 210 mins. During this time, the solutions gradually started to darken to a degree depending on the FMT concentration. Any further reaction after incubation (e.g. slow oxidation of the thiol in air) was then quenched with 33.3µls of neat acetic acid and the test solution allowed to stand for a further 30 mins. Alongside the test sample a reference solution consisting of 1ml of DMSO was prepared and treated in the same way as the test sample. The UV absorption of both the test and reference samples were then measured. We found the absorption at 300nm (after subtracting the reference sample absorption) to be the most reliable wavelength for quantitative determinations. Triethylamine could be used as an alternative to NaOH, but the latter was found to be satisfactory provided the solutions were well mixed.

The assay was first calibrated, using the same protocol, taking a number of fresh 1ml FMT/DMSO solutions of known concentrations (0.1 ml of FMT in 300 ml DMSO with relative dilutions from 1 to

0.0033) and measuring the 300nm absorptions. Figure S5 shows a calibration data set using the above protocol.

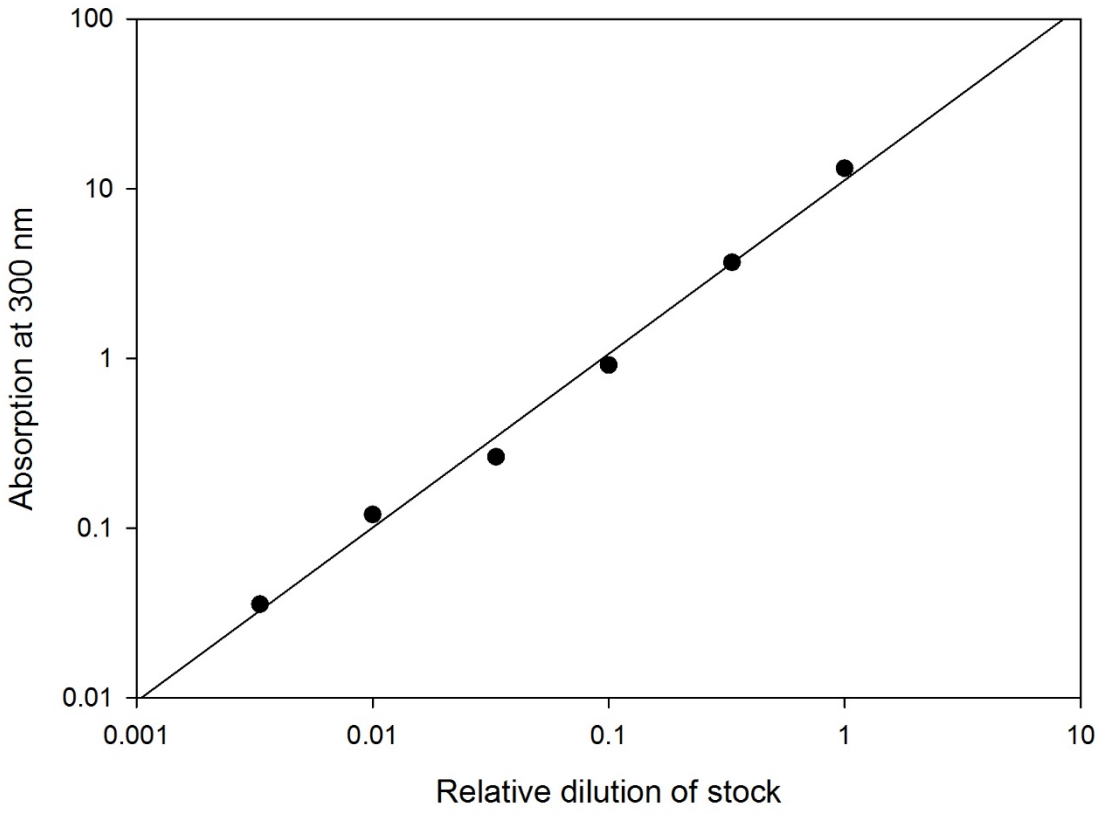


**Figure S6**. Calibration of the FMT assay method. Portions of a stock solution (0.1ml of FMT dissolved in 300 ml DMSO) were diluted by known amounts and their absorptions at 300nm wavelength measured to construct a calibration scale.

For the flow loss measurements we derived 1/e concentration decay rates for three different flow rates (25%, 40% and 60%), though in practice all of the syntheses used only 25% flow rate (100% corresponds to 1.4 l/min). The FMT concentration vs. time profiles are shown in figure S6(a) and the variation of the decay times with flow rate are shown in figure S6(b). The decay constant at the relevant flow rate was used to determine the amount of FMT lost during a reaction iteration (the reaction times are set by a LabView control program) and this was used to calculate the ideal amount of FMT to be added at the start of the next step of the reaction to compensate for the loss of ligand. This

top-up ligand was added from a diluted stock in a syringe pump by injection of a programmed volume through a catheter into the reaction flask.

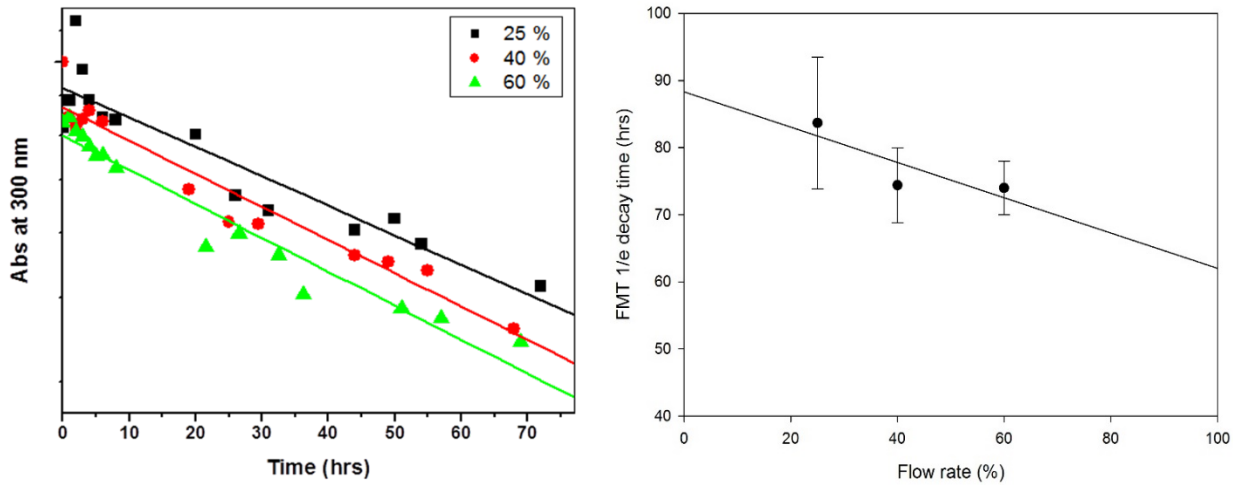


**Figure S7**. (a) FMT concentration decay profiles for three different Ar gas flow rates through a 300ml volume reaction flask. (b) Variation of the 1/e FMT depletion times vs. Ar flow rate.

**SI.5 Synthesis conditions used for samples**

Table S1. $Hg^{2+}$: ligand ratios used in this study. For runs 1 to 4 the ligand: $Hg^{2+}$ ratios were varied whilst all other conditions remained the same. For runs 5 to 7 the FMT:$Hg^{2+}$ ratio was held constant whilst the $H_2Te$ injection rate was varied. In all cases, the first reaction step consisted of a 3 minutes duration of $H_2Te$ generation at 100mA followed by a wait period of 30 minutes before a sample was taken and the next iteration was started. The current used in the subsequent steps is given in the table.

| Synthesis run number | Nominal ligand :Hg ratio | Current (mA) - Growth | mmol ligand | Hg acetate (mg) |
|---|---|---|---|---|
| 1 | 5:1 | 15 | 1.98 | 126 |
| 2 | 3:1 | 15 | 1.19 | 128 |
| 3 | 2:1 | 15 | 0.79 | 127 |
| 4 | 1.6 :1 | 15 | 0.64 | 128 |
| 5 | 2:1 | 15 | 2.37 | 375 |
| 6 | 2:1 | 30 | 2.37 | 388 |
| 7 | 2:1 | 50 | 2.37 | 352 |

**SI.6 Energy scaled representation of figure 1.**

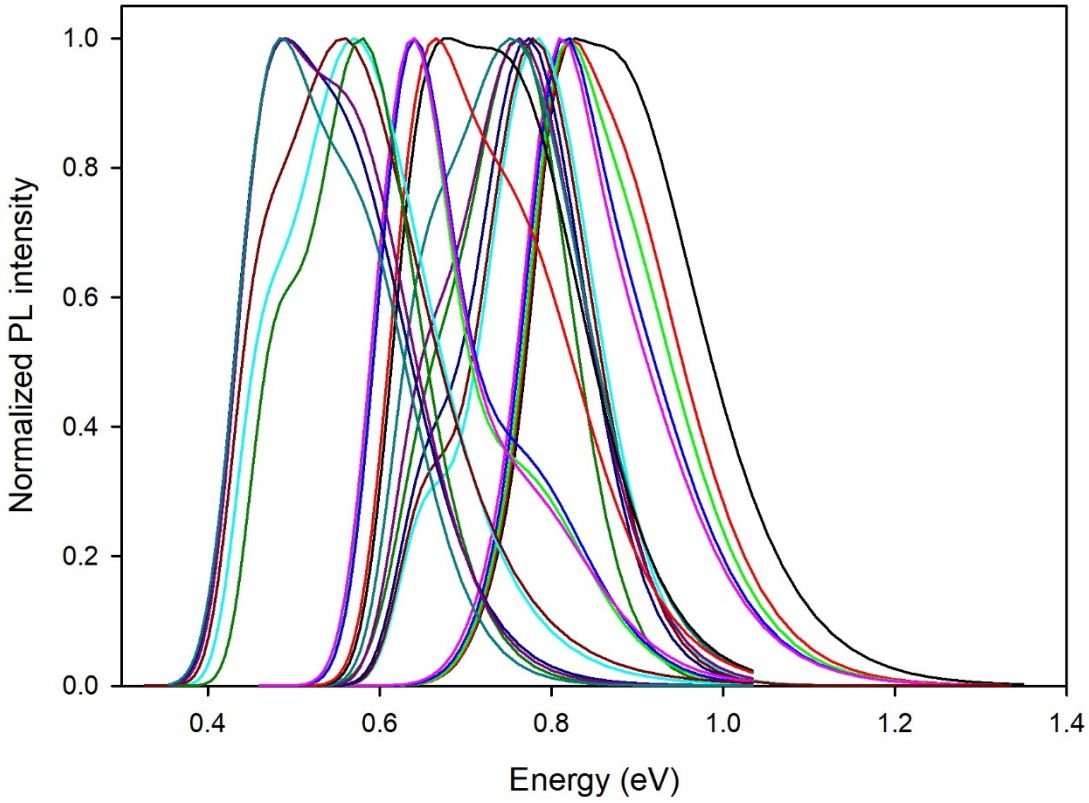


**Figure S8.** Energy scaled version of figure 1 by making the proper Jacobian transformation, $\lambda \rightarrow E$ and $I(E) = I(\lambda)/E^2$. The spectra are then represented with constant energy bandwidth for each point. With broader spectra, as here, this makes a slight change to the peak shapes than if the wavelength to energy transformation alone is made.

**SI.7 PL curve fitting example**

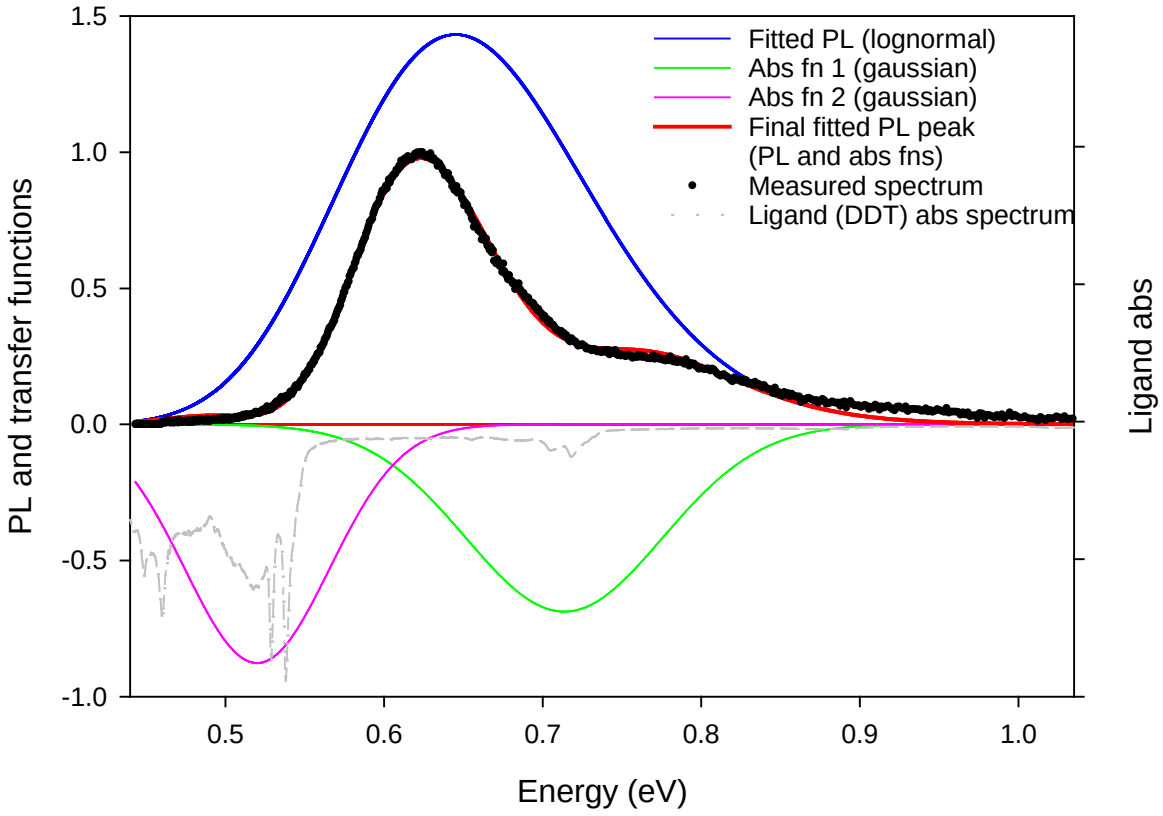


**Figure S9.** Example of using a lognormal PL fitting function with two Gaussian coupling functions representing energy transfer processes associated with vibrational modes in the DDT ligand present on the surface of the HgTe QDs. The ligand absorption spectrum is shown inverted in grey for reference.

**SI.8 HRTEM size measurements**

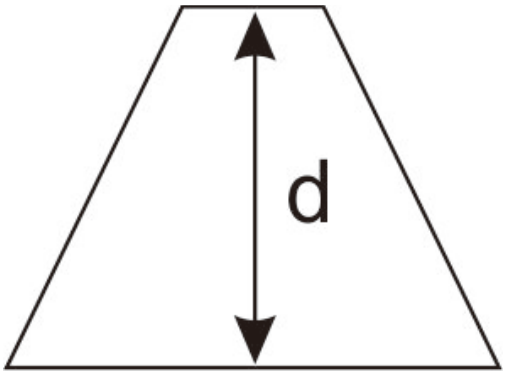


**Figure S10.** Where HRTEM images of the QDs show the QDs to be truncated pyramids, the diameter is taken to be the perpendicular distance between the face corresponding to a missing corner and the opposite side.

**SI.9 DLS monitoring of hydrodynamic sizes of HgTe QDs for different electrolysis currents**

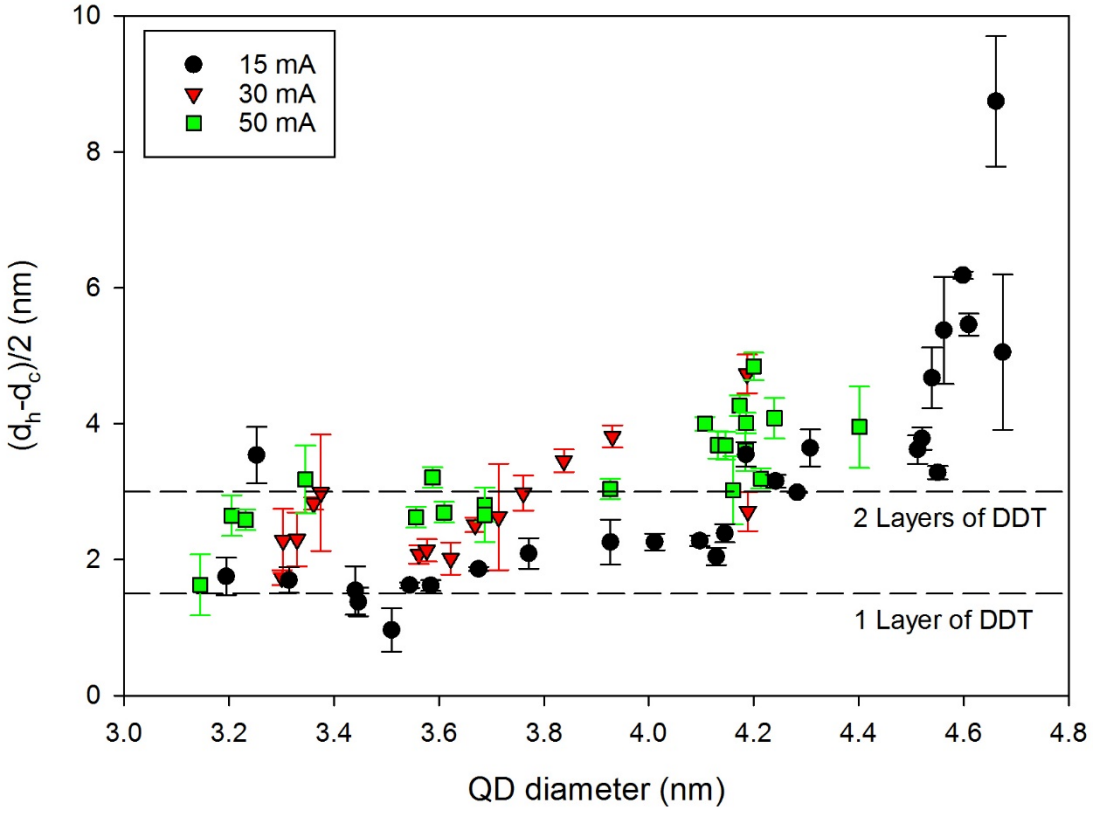


**Figure S11.** DLS measurements of the hydrodynamic shell thickness vs. HgTe QD diameter (after extraction into TCE/DDT solutions) for three synthetic runs with $H_2Te$ electrolysis currents of 15 mA, 30 mA, and 50 mA. For the slowest growth rate (15 mA) the onset of probable QD aggregation can be seen for larger particle sizes.

**SI.10 Variation in QD/ ligand coupling arising from different growth conditions as seen in PL spectra**

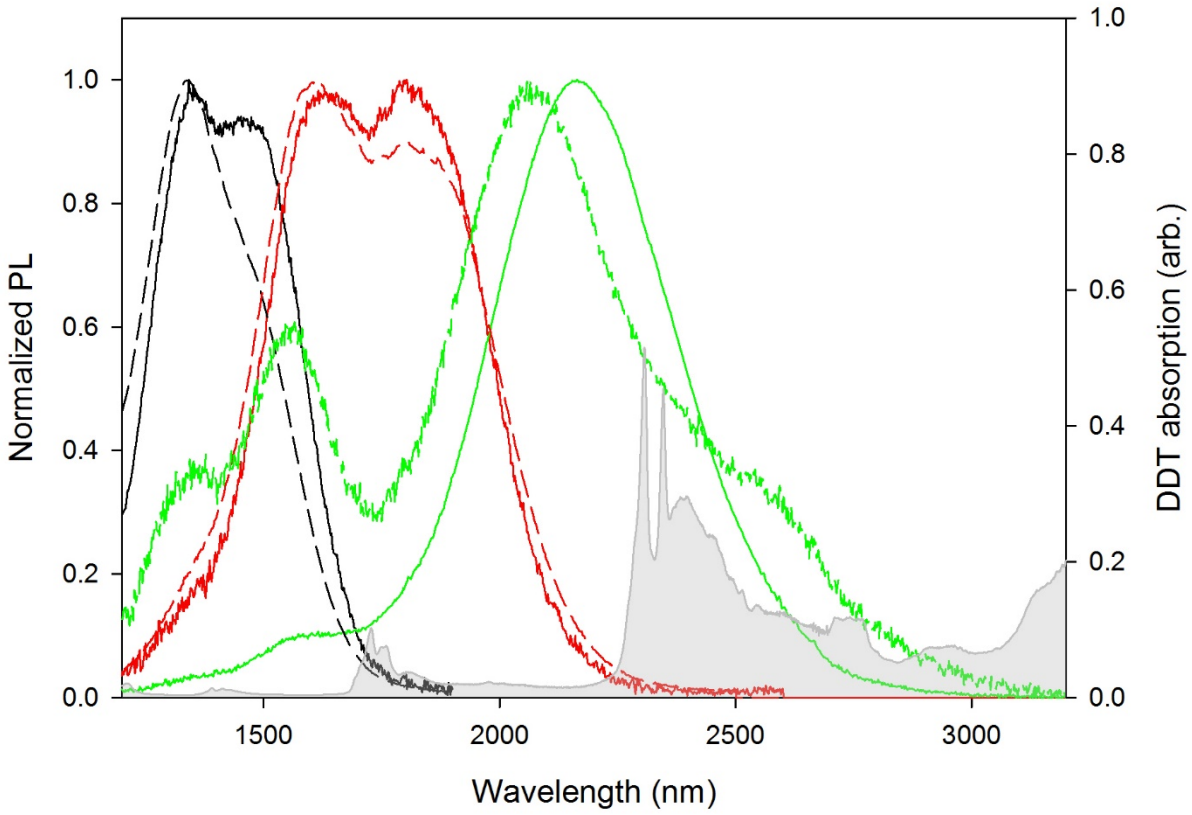


**Figure S12.** Comparisons of normalized PL spectra of HgTe QDs for the 15 mA (solid lines) and 50 mA (dashed lines) batches for aliquots that show emission in the vicinity of DDT ligand vibration bands (grey filled curve). Very heavy suppression of the 50 mA batch, longest wavelength aliquot emission above 2300nm (green dashed line) makes the short wavelength emission for that sample appear proportionately stronger after normalization.

**References.**


1. Egwim, I.O.C. and H.J. Gruber, Spectrophotometric Measurement of Mercaptans with 4,4′-Dithiodipyridine. *Anal. Biochem.* **2001**, *288*, 188-194.